

On the possibility of self-excited oscillations in a gas due to light-induced drift

F. Kh. Gel'mukhanov and T. I. Privalov

Institute of Automation and Electrometry, Siberian Branch, Russian Academy of Sciences, 630090, Novosibirsk, Russia

(Submitted 21 June 1994)

Zh. Eksp. Teor. Fiz. **107**, 140–152 (January 1995)

A nonlinear theory is presented for light-induced drift (LID) in the region where the drift velocity has an anomalous temperature dependence and changes sign with increasing temperature. It is shown for the first time that the anomalous temperature dependence of the LID velocity leads to self-excited oscillations in the concentration of the absorbing gas and in the temperature. © 1995 American Institute of Physics.

1. INTRODUCTION. TEMPERATURE DEPENDENCE OF DRIFT VELOCITY

Of the various mechanisms by which light affects the translational degrees of freedom of particles, the phenomenon of light-induced drift (LID) enjoys a unique position.¹ LID arises when optically active atoms (or molecules) in a mixture with a buffer gas are excited by resonant radiation. As a result of the velocity-selective interaction with a traveling light wave, oppositely-directed flows of excited and unexcited particles form. These experience different friction from the buffer gas and do not compensate one another because of the difference in the cross sections on the buffer particles. As a result, the absorbing gas begins to drift as a whole. For an LID velocity \mathbf{u} , we have approximately (Refs. 2, 3).

$$\mathbf{u} = -\eta \frac{\mathbf{k} \Omega}{k k} \frac{\nu_1 - \nu_0}{\nu_0}, \quad (1.1)$$

where \mathbf{k} is the radiation wave vector; $\Omega = \omega - \omega_0$ is the offset between the radiation frequency ω and the resonant frequency of the absorbing particle ω_0 ; η is the fraction of the absorbing particles that are excited but have not yet undergone velocity-changing collisions; ν_1 and ν_0 are the transport collision rates of the excited and unexcited particles, respectively. The state of the art in experimental and theoretical studies of this effect is covered in Refs. 2 and 3.

Numerical LID studies in alkali metal vapors⁴ have shown that the relative difference between the transport collision rates, $(\nu_1 - \nu_0)/\nu_0$, can change sign as the gas temperature T varies near a certain critical temperature T_c . This temperature dependence of the factor $(\nu_1 - \nu_0)/\nu_0$ was first noted by Pen'kin and Red'ko⁵ in their study of the diffusion of metastables.

As an illustration of this dependence, we consider the following model. Suppose that as the atom absorbs a photon, an electron is excited from a state 0 to an outer shell 1, far from the core. Since shell 1 screens the nuclear charge to a lesser extent than shell 0, it follows that the core is smaller in excited state 1 (Fig. 1b) than in its ground state 0 (Fig. 1a). In accord with the uncertainty principle, the scattering cross section decreases with the energy of the colliding particles (or the gas temperature). This means that at low temperatures the transport scattering cross section is determined by the

size of the outermost electron orbital. The above argument, together with Fig. 1b, suggest that $\nu_1 - \nu_0 > 0$ at low temperatures. With increasing temperature, the colliding particles begin to be scattered primarily by the inner part of the atom, i.e., by its core. Since the size of the atomic core decreases upon excitation (Fig. 1), the transport collision rate at high temperatures also decreases ($\nu_1 - \nu_0 < 0$). The equation $\nu_1 = \nu_0$ determines the so-called critical temperature T_c , at which the drift velocity \mathbf{u} vanishes.

We see from Eq. (1.1) that the anomalous temperature dependence of the factor $(\nu_1 - \nu_0)/\nu_0$ leads to an anomalous temperature dependence of the drift velocity \mathbf{u} . In fact, close to the critical temperature T_c the LID velocity \mathbf{u} will also change sign,

$$u = \alpha(T - T_c), \quad \alpha = \left[\frac{\partial u}{\partial T} \right]_{T=T_c}. \quad (1.2)$$

The existence of a critical temperature T_c has fairly recently been demonstrated in LID experiments on molecular gases.⁶

The purpose of this paper is to investigate the effect of the anomalous temperature dependence of the drift velocity, Eq. (1.2), on LID dynamics. It will be shown that close to the critical temperature T_c , the stationary state of the absorbing gas is unstable, and self-excited oscillations can occur in the gas temperature and the absorbing gas concentration. The reason for this effect is the nonlinear density-temperature relationship in the absorbing gas.

2. QUALITATIVE DISCUSSION OF SELF-EXCITED OSCILLATIONS IN A CELL WITH CLOSED ENDS

Consider a long, narrow cell with a gas mixture consisting of an absorbing and a buffer component at an ambient temperature T_a . The large ratio of the cell length L to the cross sectional radius R makes it possible to limit discussion to a one-dimensional picture, by considering that all the quantities of interest depend only on time t and the coordinate x along the axis of the cell.

Let the gas temperature T at the instant of radiation be equal to the critical temperature T_c . In that case, by virtue of (1.2) there is no drift ($\mathbf{u} = 0$), and the concentration of the absorbing component is equal to its equilibrium value n_0 . However, under certain conditions such a drift-free state of

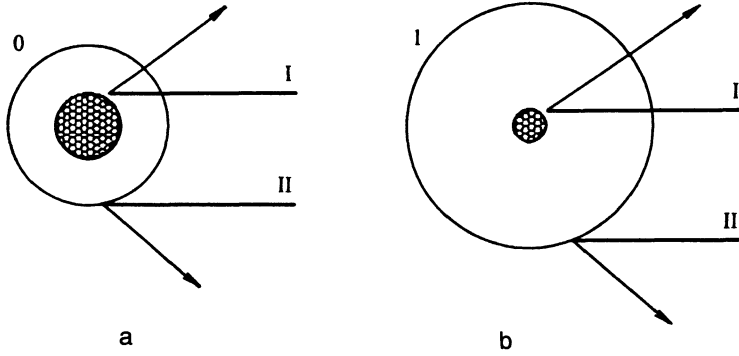


FIG. 1. Schematic representation of the temperature dependence of the velocity drift: a) ground-state atom, b) excited atom. The marked region is the atomic core, the circle is the outer electron orbital. At high energies (temperatures), the buffer particles are scattered by the core (trajectory I), whereas at low energies (temperatures), the cross section increases and is determined by the size of the outer electron orbit (trajectory II).

the gas is one of unstable equilibrium. Suppose at the left-hand end of the gas-filled cell there is a concentration perturbation $\delta n(x) = n(x) - n_0$ (Fig. 2). The fact that $\delta n(x)$ can change sign follows from the conservation of the number of particles in the cell. Owing to photoabsorption, with a subsequent thermalization of the excitation energy, region A (Fig. 2) is heated. In its turn, the temperature in region B decreases. As a result, the drift velocity (1.2) becomes non-zero, with $u > 0$ in region A and $u < 0$ in B, for $\alpha > 0$.

Let us introduce a characteristic heat exchange time t_{ex} with the ambient medium, and a drift displacement time $t_u = l/u \approx D/u^2$ corresponding to a characteristic distance l of the order of the packet width ($l \approx D/u$, D being the diffusion coefficient for the absorbing particles in the buffer gas). Clearly, for $t_{ex} \ll t_u$, the drift-free state of the gas will be stable.

For a finite heat exchange rate,

$$t_{ex} \geq t_u, \quad (2.1)$$

the situation is qualitatively different. In fact, owing to the rapid (drift-velocity) motion of a temperature nonuniformity along the cell axis, the gas does not have time to relax to the equilibrium temperature T_c . In that case region A (Fig. 2), where $u > 0$, will move to the right while suffering deformation, but will remain undamped, whereas region B will move

to the left. The leftward drift of particles out of B will lead to a particle pile-up at the left-hand end of the cell. The result is that after some time, $\delta n(x, t)$ close to the left-hand end will be positive, and hence so will the drift velocity ($u > 0$). In other words, near the left-hand end a new condensation forms which starts drifting to the right. The above discussion implies that the criterion (2.1) is in fact an instability condition for a spatially uniform distribution of concentration and temperature in the absorbing gas.

The above qualitative arguments demonstrate the initial stage in the development of the stationary periodic LID regime (Fig. 2).

We now proceed to a quantitative description of this effect.

3. NONLINEAR THEORY OF LID. HEAT EXCHANGE WITH THE AMBIENT MEDIUM. ANOMALOUS TEMPERATURE DEPENDENCE OF LID VELOCITY

As already noted, we restrict attention to a one-dimensional description in which all physical quantities depend only on the longitudinal coordinate x parallel to the drift velocity.

The concentration of absorbing gas particles n obeys the continuity equation

$$\frac{\partial n}{\partial t} + \frac{\partial j}{\partial x} = 0, \quad (3.1)$$

where the absorbing particle flux, using the drift velocity expression (1.2), is given by

$$j = \alpha \tau n - D \frac{\partial n}{\partial x}.$$

Taking into account the strong dependence of the flux j on the gas mixture temperature T , Eq. (3.1) must be supplemented the well-known thermal balance equations for the gas

$$\rho c \frac{\partial T}{\partial t} = \kappa \frac{\partial^2 T}{\partial x^2} - b(T - T_w) + n \sigma K I, \quad (3.2)$$

and for the side walls of the absorbing cell at temperature T_c ,

$$\rho_w c_w \frac{\partial T_w}{\partial t} = \kappa_w \frac{\partial^2 T_w}{\partial x^2} - b'(T - T_a) - b(T_w - T), \quad (3.3)$$

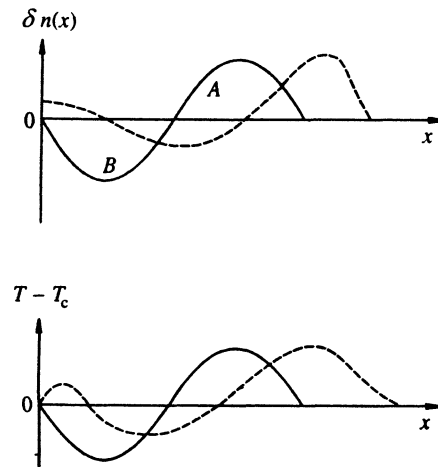


FIG. 2. Qualitative development of self-excited oscillations in the domain of anomalous temperature dependence of the drift velocity, Eq. (1.2).

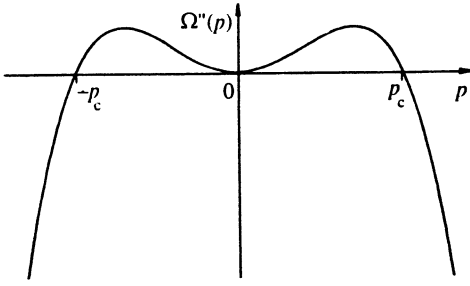


FIG. 3. Instability damping factor Ω'' in Eq. (4.7) as a function of wave number ρ .

where ρ , c , and κ are the gas mixture mass density, specific heat, and thermal conductivity, respectively; ρ_w , c_w , and κ_w , the same for the wall material; b and b' are the heat exchange coefficients respectively between the gas mixture and the side wall and between the wall and the environment at T_a ; σ is the photoabsorption cross section. In deriving Eqs. (3.2) and (3.3) we have taken into account Lambert's law for the radiative intensity I ,

$$\frac{\partial I}{\partial x} = -n\sigma I, \quad (3.4)$$

along with the heat flux along the side walls, $q_w = -\kappa_w \partial T_w / \partial x$, and the total energy flux of the gas mixture, $q = -\kappa \partial T / \partial x + KI$, which is the conventional heat flux plus the Poynting vector (the radiative intensity) I . The coefficient K denotes the fraction of the radiative energy absorbed by the gas that is transformed into thermal energy.

The low gas density and thermal conductivity, compared to ρ_w and κ_w for the wall material, enable one to replace Eq. (3.2) with

$$T = T_w + n\sigma KI/b.$$

To simplify the description, we make two further approximations that are devoid of any fundamental significance: 1) we consider only an optically thin medium ($L\sigma n_0 \ll I$), and 2) heat exchange between the walls and the external medium is taken to be small compared to that between the walls and the absorbing gas, that is, $\varepsilon b'/b \ll I$, where

$$\varepsilon = \frac{I^2 \alpha(I_0) n_0 \sigma K t_{ex}}{I_0 \rho_w c_w \sqrt{D/t_{ex}}}. \quad (3.5)$$

In this last relation we have assumed that the parameter α of Eq. (1.2) is a linear function of the radiative intensity [$\alpha = \alpha(I) = \alpha(I_0)I/I_0$], and that the radiative intensity does not exceed its saturation value I_{sat} , where I_0 is some fixed intensity. With this understanding, and introducing the dimensionless parameters

$$\tau = \frac{t}{t_{ex}}, \quad z = \frac{x}{\sqrt{D t_{ex}}}, \quad N = \frac{n}{n_0}, \quad \Theta = \frac{\alpha(T_w - T_c)}{\sqrt{D/t_{ex}}}. \quad (3.6)$$

Eqs. (3.1) and (3.3) can be rewritten in the form

$$\frac{\partial N}{\partial \tau} + \frac{\partial(N\Theta)}{\partial z} = \frac{\partial^2 N}{\partial z^2}, \quad (3.7)$$

$$\frac{\partial \Theta}{\partial \tau} = \Delta \frac{\partial^2 \Theta}{\partial z^2} - \Theta + \varepsilon N + \Theta_a, \quad (3.8)$$

where

$$\Delta = \frac{\chi}{D}, \quad \chi = \frac{\kappa_w}{\rho_w c_w}, \quad t_{ex} = \frac{\rho_w c_w}{b'}, \quad \Theta_a = \frac{\alpha(T_a - T_c)}{\sqrt{D/t_{ex}}}. \quad (3.9)$$

As we shall see below, the dimensionless parameters Δ , Eq. (3.9), and ε , Eq. (3.5), will determine the nontrivial nature of LID dynamics under the conditions of the anomalous temperature dependence (1.2). For a finite cell, this set of equations must be supplemented by boundary conditions for N and Θ at the ends of the cell. The corresponding boundary conditions will be discussed below (see Sec. 6).

4. STABILITY ANALYSIS FOR THE STATIONARY, SPATIALLY UNIFORM SOLUTION IN AN UNBOUNDED MEDIUM. NEUTRAL CURVE

For an unbounded cell the stationary and spatially uniform solution of the set of Eqs. (3.7) and (3.8) is obvious:

$$N_0 = 1, \quad \Theta_0 = \Theta_a + \varepsilon. \quad (4.1)$$

Conditions for the existence of a solution of Eq. (4.1) for a finite cell with associated boundary conditions are given below (Sec. 6).

We analyze the stationary solution (4.1) for stability by introducing the deviations N' and Θ' ,

$$N = 1 + N', \quad \Theta = \Theta_0 + \Theta'. \quad (4.2)$$

The present work is restricted to the case

$$\Theta_0 = 0, \quad (4.3)$$

i.e., the side wall temperature in a stationary and spatially uniform state is assumed to be equal to the critical temperature T_c , Eq. (1.2).

We next assume small deviations from the stationary solution (4.1) and linearize Eqs. (3.7) and (3.8). Solutions of the resulting linearized equations are assumed to take the form

$$\exp(-i\Omega\tau + ipz), \quad (4.4)$$

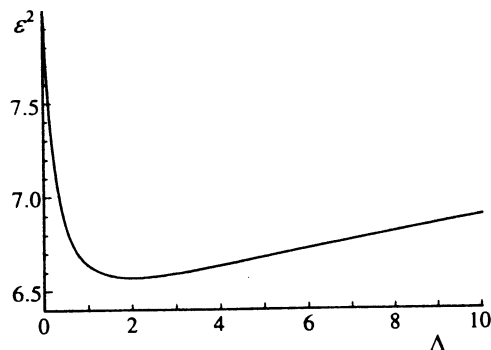


FIG. 4. Neutral curve. II is the domain of absolute instability.

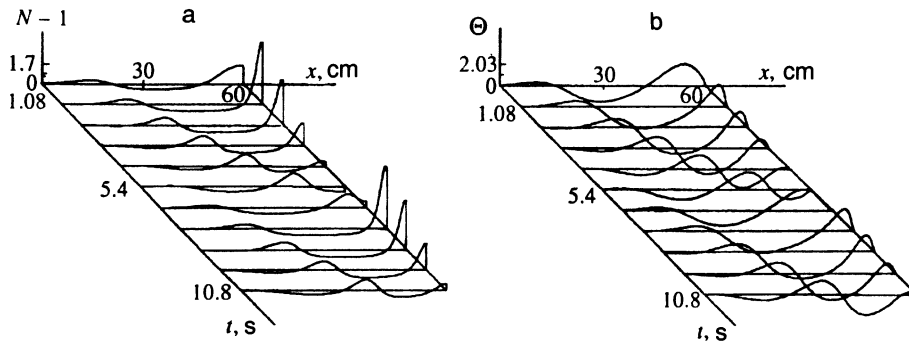


FIG. 5. Steady-state oscillations of the spatial distribution of a) dimensionless absorptive component concentration N , Eq. (3.7); b) temperature Θ , Eq. (3.8). $L=60$ cm. The remaining parameters are the same as in Eq. (6.5).

yielding the dispersion relation

$$\Omega^2 + i\Omega[(1+\Delta)p^2 + 1] - p^2(1+\Delta p^2) - i\epsilon p = 0. \quad (4.5)$$

The dimensionless frequency Ω is a complex quantity,

$$\Omega = \Omega' + i\Omega''.$$

Here we only give the solution of the dispersion relation (4.5) for the unstable branch,

$$\Omega' = \epsilon p [1 - (1+\Delta)p^2], \quad (4.6)$$

$$\Omega'' = -\epsilon^2(3\Delta + 2)p^2(p^2 - p_c^2), \quad (4.7)$$

obtained in the long-wavelength limit

$$p \ll 1, \quad (4.8)$$

In Eqs. (4.6) and (4.7) the following notation has been used:

$$p_c^2 = \frac{\epsilon^2 - 1}{3\Delta + 2}. \quad (4.9)$$

We see from Eq. (4.9) that if

$$\epsilon^2 > 1, \quad (4.10)$$

then in the long-wavelength region (Fig. 3)

$$|p| < p_c \quad (4.11)$$

the stationary solution (4.1) becomes unstable ($\Omega'' > 0$).

Neutral curve

The fact that the dispersion relation (4.5) has roots in the upper half of the Ω plane implies that a small initial perturbation (4.4) in an infinitely long cell builds up exponentially, i.e., the system is unstable.

For an unbounded system there are two possibilities. In the first, an initial perturbation in the form of a wave packet of finite spatial dimensions builds up everywhere in space; this is known as an absolute instability. If the packet is transported along the cell so rapidly that the perturbation everywhere tends to zero as $t \rightarrow \infty$, then the instability is of the convective type.⁷

To determine the domain of absolute instability, we rewrite the dispersion relation (4.5) as an equation in p :

$$\Delta p^4 + [1 - i\Omega(1+\Delta)]p^2 + i\epsilon p - i\Omega - \Omega^2 = 0. \quad (4.12)$$

According to Ref. 7, the values of Ω determining the nature of the instability are chosen from among those Ω for which

two roots of the dispersion relation (4.12), p_1 and p_2 , coalesce ($p_1 = p_2$) at a certain frequency $\Omega = \Omega_c$, whereupon the dispersion relation becomes

$$\Delta(p-p_1)^2(p-p_3)(p-p_4) = 0, \quad (4.13)$$

where p_3 and p_4 are the two remaining roots. Comparison of Eqs. (4.12) and (4.13) allows one to determine the Ω_c at the merger point. The domain of absolute instability is bounded by the so-called neutral curve in the (ϵ^2, Δ) plane, on which $\Omega_c'' = 0$. The parametric equation of the neutral curve

$$x^3(\Delta-1)^4 + x^2 2(2\Delta-5)(\Delta-1)^2 + x \left[5 - 4\Delta + \epsilon^2 \right. \\ \left. \times \left(9 - \frac{33}{4}(1+\Delta)^2 \right) \right] + 0.25\epsilon^2 \left(1 - \frac{27}{4}\Delta\epsilon^2 \right) = 0, \quad (4.14)$$

$$x^2(\Delta-1)^3(5-\Delta) + x[2(\Delta-1)(3\Delta-5) + \epsilon^2(\Delta+1) \\ \times (1-34\Delta+\Delta^2)0.25] - 1 + \frac{3}{4}\epsilon^2(11\Delta-1) = 0 \quad (4.15)$$

follows directly from Eqs. (4.12), (4.13), and the condition ($\Omega_c'' = 0$). Here $x = \Omega^2 > 0$, $\Omega'' = 0$.

Equations (4.14) and (4.15) can be solved analytically for $\Delta=0$ and $\Delta \gg 1$, giving

$$\epsilon^2 = 8, \quad x = 1, \quad \text{for } \Delta = 0, \epsilon^2 = 8 - 40\Delta^{-1}, \\ x = 2\Delta^{-1}(1 - 20\Delta^{-1}), \quad \text{for } \Delta \gg 1. \quad (4.16)$$

For the intermediate range of the parameter Δ , Eqs. (4.14) and (4.15) were solved numerically. The results are given in Fig. 4.

The present derivation of the neutral curve (4.14)–(4.15) suffers from one major drawback. We have not proven the second necessary criterion for absolute instability, namely that when the roots p_1 and p_2 leave the neutral curve, they deviate from one another and wind up on opposite sides of the real axis in the p plane for $\Omega'' \rightarrow \infty$ (Ref. 7). To remedy this problem, an alternative, rigorous but more cumbersome derivation was carried out, based on a direct determination of the roots of the dispersion relation (4.12) using the Ferrari

method.⁸ As a result, we were able to show that the parametric equations (4.14) and (4.15) are indeed the equations of the neutral curve.

To find out whether the region of absolute instability lies above or below the neutral curve (4.14)–(4.15), we explored numerically the merger of the roots $p(\Omega)$ of (4.12), the positions of the roots being determined by the Ferrari method. It was found that above (below) the curve the merger occurs for $\Omega'' > 0$ ($\Omega'' < 0$). Thus, in the region above the neutral curve (Fig. 4) the system is absolutely unstable.

5. INSTABILITY OF A FINITE-LENGTH SYSTEM

The problem of analytically determining the domain of instability of a finite-length system is a difficult one. The reason for this is the complication brought about by the boundary conditions. The instability criterion begins generally to depend on the length L as well. A finite-size system is unstable if its length \bar{L} exceeds a certain critical value L_c ,^{7,9}

$$\bar{L} > L_c(\varepsilon^2, \Delta), \quad (5.1)$$

which depends on the parameters ε^2 and Δ involved in the problem (3.7)–(3.8) under study. Here we have introduced the dimensionless cell length

$$\bar{L} = L / \sqrt{D/t_{\text{ex}}}.$$

Unfortunately, we have been unable to find a rigorous analytic expression for the critical cell length L_c .

We shall present here some qualitative arguments allowing a rather accurate estimate of the dimensionless critical cell length $L_c(\varepsilon^2, \Delta)$ [see Eq. (5.1)]. From the definition (5.1), the length L_c does not depend directly on the cell length (even though the function $L_c(\varepsilon^2, \Delta)$ is generally dependent on the boundary conditions); hence, it is a characteristic of the unbounded medium. But the only spatial scale available in the stability analysis of an infinite cell is $2\pi/p_c$, where p_c is

the critical wave vector; see Eq. (4.9). With no loss of generality, the expression for the critical length L_c can be cast in the form

$$L_c = n \frac{2\pi}{p_c}, \quad (5.2)$$

where $n = n(\Delta, \varepsilon^2)$ is in general some function of the parameters Δ and ε^2 . It is natural to assume that $n \approx 1$ and that it depends weakly on Δ and ε^2 . To test this assumption we solved Eqs. (3.7) and (3.8) numerically for the boundary conditions (6.1) and (6.2) (with $\Theta = 0$) for various dimensionless lengths \bar{L} . We defined L_c as the critical length beyond which the cell develops oscillations, and before which the solution tends to a stable, spatially uniform one. Calculations indicate that $n \approx 3$.

Thus, we suggest the following approximate formula for the dimensionless critical length L_c :

$$L_c(\varepsilon^2, \Delta) = 3 \frac{2\pi}{p_c} = 6\pi \sqrt{\frac{3\Delta + 2}{\varepsilon^2 - 1}}, \quad (5.3)$$

above which ($\bar{L} > L_c$) the system is unstable.

Additional studies indicate that the semi-empirical formula (5.3) agrees fairly well with a direct numerical solution of the nonlinear equations (3.7) and (3.8).

6. SELF-EXCITED OSCILLATORY REGIME IN A CELL WITH CLOSED ENDS

The nonlinear equations (3.7) and (3.8) have not lent themselves to analytic solution, and were therefore solved numerically, subject to appropriate boundary conditions at the ends of the cell.

The first two boundary conditions express the absence of any flux of absorbing gas through the ends:

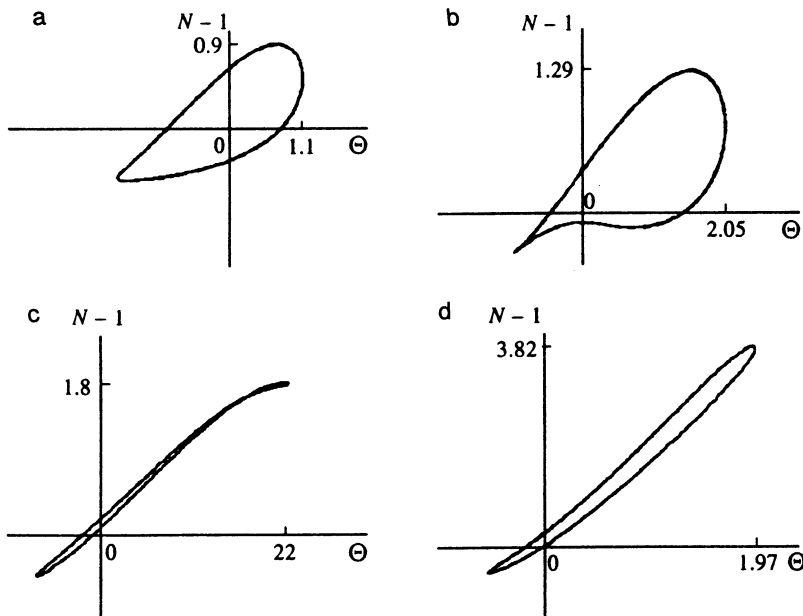


FIG. 6. Limit cycles corresponding to the solution in Fig. 5 for various points in the cell: a) $x/L=0.5$; b) $x/L=0.9$; c) $x/L=0.95$; d) $x/L=0.97$.

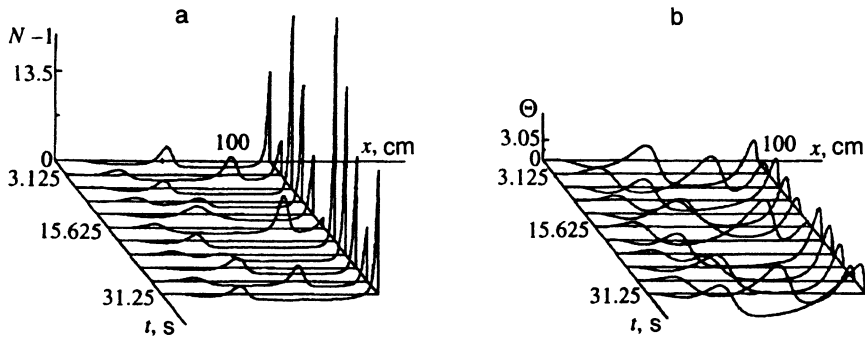


FIG. 7. As in Fig. 5, for $L=100$ cm.

$$\left[\Theta(z, \tau) N(z, \tau) - \frac{\partial}{\partial z} N(z, \tau) \right]_{z=0, \bar{L}} = 0. \quad (6.1)$$

The second pair of boundary conditions is dictated by the nature of heat exchange at the ends. The present work is limited to the two simplest possibilities:

$$\Theta(z, \tau)|_{z=0, \bar{L}} = \tilde{\Theta}, \quad (6.2)$$

$$\frac{\partial}{\partial z} \Theta(z, \tau)|_{z=0, \bar{L}} = 0, \quad (6.3)$$

where $\tilde{\Theta}$ is the end value of $\Theta(z, \tau)$. The numerical solution of Eqs. (3.7) and (3.8) was carried out by setting $\tilde{\Theta}=0$. This condition implies that the side wall temperature T_w at the ends of the cell is equal to the critical temperature T_c , whereas the second type of boundary condition, Eq. (6.3), corresponds to a lack of thermal flux across the ends. The choice $\tilde{\Theta}=0$ implies further that the stationary solution (4.1) and (4.3) also satisfies boundary conditions like (6.2)–(6.3), and corresponds to a side wall temperature

$$T_w = T_c = T_a + \varepsilon \alpha^{-1} \sqrt{D/t_{ex}}, \quad (6.4)$$

which is equal to the end temperature.

Figures 5a and 5b show the solution of Eqs. (3.7) and (3.8) with boundary conditions (6.1) and (6.2) in the steady-state regime, for $L=60$ cm and parameter values

$$\Delta = 1, \quad \varepsilon^2 = 20, \quad (6.5)$$

$$b = 1 \text{ s}^{-1}, \quad \alpha = 1 \text{ cm/s}\cdot\text{K} \quad D = 20 \text{ cm}^2/\text{s}.$$

The parameters Δ and ε^2 lie above the neutral curve (Fig. 4). The corresponding spatial distributions of N and Θ are given for various times (with the same interval along the time axis). The solution represents condensations of the absorbing gas traveling from the left to the right end of the cell. We see from Figs. 5a and 5b that this choice of L , Δ , and ε^2 in Eq. (6.5) leads to the self-excited oscillatory regime (independent of the particular choice of boundary conditions). A more transparent confirmation of the approach of the above solution to a steady-state self-excited oscillatory regime is provided by the limit cycle of the solution of Eqs. (3.7) and (3.8) in the middle of the cell; see Fig. 6a. The phase trajectory of this solution (Fig. 6a) is closed, attesting to the strict periodicity of the observed self-excited oscillations. Note that the form of the limit cycle of the observed periodic solution of Eqs. (3.7) and (3.8) depends on the observation point. Fig-

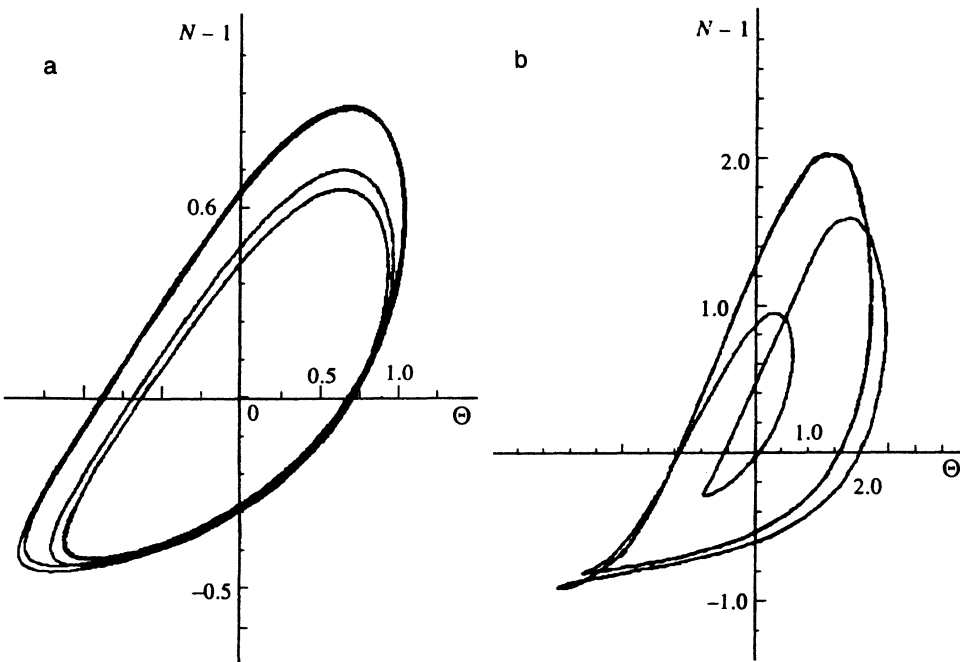


FIG. 8. Limit cycles corresponding to the solution in Fig. 7 for various points in the cell: a) $x/L=0.25$; b) $x/L=0.5$.

ures 6a, b, c, and d, respectively, show phase trajectories in the middle of the cell and at points 0.9, 0.95, and 0.97 times the cell length from the beginning of the cell.

Such behavior has also been seen for other values of ε , Δ , and L in the domain of instability (5.3); see Fig. 4. The solution became more complicated as the cell length increased, in that the number of absorbing-gas condensations increased, and the phase trajectory exhibited a multiperiodic behavior in contrast to Fig. 6. The results of a numerical solution of Eqs. (3.7) and (3.8) for a cell length of $L=100$ cm [the remaining parameters being as in Eq. (6.5)] are presented in Figs. 7a and 7b. The phase portrait of this solution at one-fourth the length and midway along the cell are given in Figs. 8a and 8b, respectively.

In both qualitative discussion and numerical work we have restricted attention to positive α [Eq. (1.2)]. According to Eq. (1.1), the sign of α depends on the sign of the frequency offset Ω . In the present work we have treated only the optically thin case, Eqs. (3.1), (3.2), and (3.3) [or Eqs. (3.7), (3.8)]. These equations are invariant under a change in sign of both the parameter α and the coordinate x ($\alpha \rightarrow -\alpha, x \rightarrow -x$). Thus, changing the sign of α is equivalent to changing the sign of the coordinate x or to reversing the laser beam propagation direction. Consequently, solution of Eqs. (3.1), (3.2), and (3.3) [or Eqs. (3.7) and (3.8)] for $\alpha < 0$ is identical to solution of the same equations with $\alpha > 0$ and reversal of the x axis (opposite radiation propagation direction).

To conclude, we estimate LID for Li vapor in the buffer gas Ne-C₂H₄. A small admixture of C₂H₄ molecules is required for the collisional transformation of a fraction of the

absorbed radiative energy into thermal energy.¹⁰ Numerical calculations for a Li-Ne system yield a critical temperature $T_c \geq 1000$ K. LID estimates for a copper cell yield $I_c \approx 10$ W/cm² and $L_c \approx 10$ cm.

The authors thank S. N. Atutov, A. I. Chernykh, G. Nienhaus, A. M. Shalagin, and E. Eliel for fruitful discussions and a number of valuable comments.

This research was supported in part by International Science Foundation Grant No. RCM000 and by a grant from the Russian Basic Research Foundation (RBRF). The financial support of the Netherlands Organization for Scientific Research and the "Universities of Russia" Program is also acknowledged.

¹F. Kh. Gel'mukhanov and A. M. Shalagin, Pis'ma Zh. Eksp. Teor. Fiz. **29**, 773 (1979) [JETP Lett. **29**, 711 (1979)].

²S. G. Rautian and A. M. Shalagin, *Kinetic Problems of Nonlinear Spectroscopy*, North-Holland, Amsterdam (1991).

³H. G. C. Werij and J. P. Woerdman, Phys. Rep. **169**, 145 (1988).

⁴A. I. Parkhomenko, Opt. Spektrosk. **67**, 26 (1989) [Opt. Spectrosc. (Russia) **67**, 14 (1989)].

⁵N. P. Pen'kin and T. P. Red'ko, in *Spectroscopy of a Gas-Discharge Plasma* [in Russian], V. 1, p. 51, LGU, Leningrad (1976).

⁶G. J. Van der Meer, *Molecular Collision Processes Studied by Light-induced Kinetic Effects*, Ph.D. Thesis, Leiden (1992).

⁷E. M. Lifshitz and L. P. Pitaevskii, *Physical Kinetics* [in Russian], Nauka, Moscow (1979).

⁸A. G. Kurosh, *A Course in Higher Algebra* [in Russian], Nauka, Moscow (1975).

⁹A. M. Fedorchenko and N. Ya. Katsarenko, *Absolute and Convective Instability in Plasmas and Solids* [in Russian], Nauka, Moscow (1981).

¹⁰M. C. de Lignie and J. P. Woerdman, J. Phys. **B23**, 417 (1990).

Translated by E. Strelchenko